Theory of Impedance Spectroscopy of Ambipolar Solar Cells with Trap-Mediated Recombination

Luca Bertoluzzi,[†] Pablo P. Boix,[‡] Ivan Mora-Sero,[†] and Juan Bisquert*,[†]

[†]Photovoltaics and Optoelectronic Devices Group, Departament de Física, Universitat Jaume I, 12071 Castelló, Spain

[‡]Energy Research Institute @NTU (ERI@N), Research Techno Plaza, X-Frontier Block, Level 5, 50 Nanyang Drive, Singapore 637553

ABSTRACT: The analysis of recombination in solar cells suggests in many cases the presence of trap-mediated recombination in the absorber. We present a theory of the recombination of electrons and holes, the Shockley–Read–Hall model, using the impedance spectroscopy technique. We derive the impedance functions and the corresponding equivalent circuit model. After examining some cases of interest, we show that two semicircles can be obtained in the recombination circuit only if the chemical capacitance associated with traps is substantially larger than the chemical capacitances of free electrons and holes in the absorber bands, while in the other cases the normal behavior of one recombination arc will be obtained.
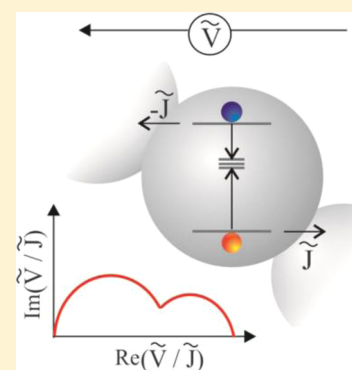
INTRODUCTION

In the fundamental operation of a solar cell, the carriers generated in the absorber are transported to distinct selective contacts for electrons and holes.[1] Ambipolar transport refers to the situation in which electrons and holes of similar number and mobilities govern the carrier transport in the semiconductor.[2] A minority carrier governs the behavior of most classes of solar cells, such as crystalline silicon solar cells and dye-sensitized solar cells, while the majority carrier is a spectator whose background density is not altered by illumination or voltage injection except in very extreme circumstances. However, recently some solar cells that display acute ambipolar characteristics have come to the forefront of research. These are the quantum dot film solar cells[3] and organometal halide perovskite solar cells.[4,5] In both classes of cells, it is likely that similar number of electrons and holes are transported simultaneously in the same medium (the absorber) toward macroscopic selective contacts. These mechanisms are currently a matter of investigation. Given the fact that the materials are prepared by low-temperature processing methods, it is likely that the semiconductor absorber contains abundant traps that will act as recombination centers for electrons and holes.

Impedance spectroscopy (IS) is a method that has become widely popular for the understanding of electronic processes and technical characterization of solar cells.[6] The theory of diffusion-recombination impedance[7] describes well the ac dynamics of solar cells dominated by single carrier transport. This technique has been extended to include the retarding effects of disordered localized levels in the bandgap as well as nonlinear recombination.[8] This model has been widely used for the description of dye-sensitized solar cells and organic solar cells.[6]

In this paper, we develop the theory of impedance spectroscopy of Shockley–Read–Hall (SRH) recombination in ambipolar semiconductors. The general small perturbation equivalent circuit model, leading to a transmission line, was first calculated by Shockley[9] and perfected by Sah[10] but to our knowledge the application to solar cells of the full impedance model has not been derived in the previous literature. Here we provide a schematic formulation of the main results and the application of the general ac model to solar cells with explicit derivation of the impedance function and a general analysis of spectral characteristics.

THEORY

We formulate a model semiconductor solar cell as shown in Figure 1. In this paper, we are mainly interested in disclosing the recombination dynamics of electrons and holes that include spectral characteristics of the separate carriers. Therefore here we simplify all transport features and we assume that carrier densities are homogeneous in the semiconductor layer of thickness L. If only direct recombination of electrons and holes is considered, the ac equivalent circuit (EC) consists on a single arc with mixed parameters of both species.[11] In order to obtain more structured spectra, it is important to consider the recombination via inner band gap traps in the SRH model, as
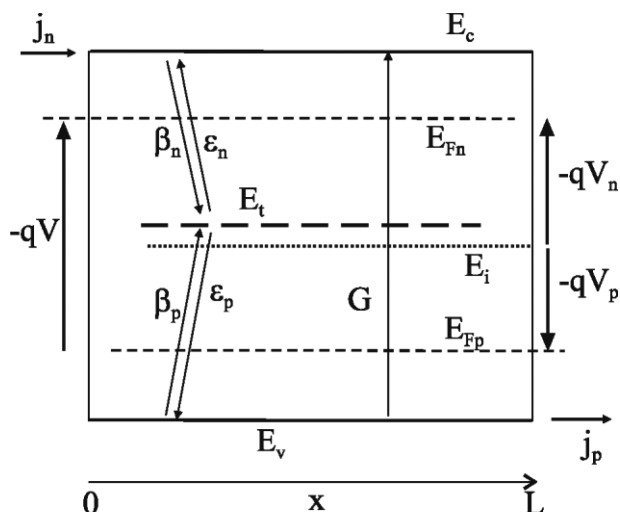
Figure 1. Ambipolar solar cell model with two selective contacts that allow injection and extraction of electrons and holes at either side and SRH recombination via a trap state in the bandgap.

shown in Figure 1. The circuit obtained in this work will become part of a transmission line in the case in which transport is considered explicitly.

In the present model, the conduction band lower edge with effective density of states N_c is at the energy E_c. The upper edge of the valence band with effective density of states N_v is at energy E_v. The recombination center is at the energy E_t with density N_t. The density of electrons n can be related to the electron Fermi level E_{Fn} according to the Boltzmann statistics

$$n = N_c e^{(E_{Fn}-E_c)/k_BT}$$

$$= n_i e^{(E_{Fn}-E_i)/k_BT} \qquad (1)$$

where k_BT is thermal energy and n_i and E_i are respectively the density and energy of the intrinsic level. Similarly for the hole density p

$$p = N_v e^{(E_v-E_{Fp})/k_BT}$$

$$= p_i e^{(E_i-E_{Fp})/k_BT} \qquad (2)$$

For the fractional occupancy of the trap, f, using a trap Fermi level E_{Ft}, we obtain

$$f = \frac{1}{1 + e^{(E_t-E_{Ft})/k_BT}}$$

$$= \frac{1}{1 + e^{(qV_\varepsilon+E_i-E_{Ft})/k_BT}} \qquad (3)$$

where $qV_\varepsilon = E_t - E_i$, being q the positive elementary charge. It is convenient to define the following voltages

$$-qV_n = E_{Fn} - E_i \qquad (4)$$

$$-qV_p = E_{Fp} - E_i \qquad (5)$$

$$-qV_t = E_{Ft} - E_i \qquad (6)$$

Therefore we can write the carrier densities as

$$n = n_i e^{-qV_n/k_BT} \qquad (7)$$

$$p = p_i e^{+qV_p/k_BT} \qquad (8)$$

$$f = \frac{1}{1 + e^{q(V_\varepsilon+V_t)/k_BT}} \qquad (9)$$

The carriers dynamics are determined by continuity equations for the three species

$$\frac{\partial n}{\partial t} = +\frac{1}{q}\frac{\partial j_n}{\partial x} + G - \beta_n N_t(1-f)n + \varepsilon_n N_t f \qquad (10)$$

$$\frac{\partial p}{\partial t} = -\frac{1}{q}\frac{\partial j_p}{\partial x} + G + \varepsilon_p N_t(1-f) - \beta_p N_t p f \qquad (11)$$

$$\frac{\partial f}{\partial t} = \beta_n(1-f)n - \varepsilon_n f + \varepsilon_p(1-f) - \beta_p p f \qquad (12)$$

Here G is a generation rate and β_k and ε_k are the capture and release coefficients, respectively, between the trap and the bands. j_n and j_p are the local electric current density of electrons and holes, respectively. The detailed balance condition[12] implies that

$$\frac{\varepsilon_n}{n_i\beta_n} = \frac{p_i\beta_p}{\varepsilon_p} = e^{(E_t-E_i)/k_BT} \qquad (13)$$

The boundary conditions associated to ideal selective contacts are

$$j_n(x=L) = j_p(x=0) = 0 \qquad (14)$$

Under the assumption that the active layer is homogeneous, we can integrate eqs 10 and 11 as follows

$$\frac{\partial n}{\partial t} = -\frac{j_n}{qL} + G - \beta_n N_t(1-f)n + \varepsilon_n N_t f \qquad (15)$$

$$\frac{\partial p}{\partial t} = -\frac{j_p}{qL} + G + \varepsilon_p N_t(1-f) - \beta_p N_t f p \qquad (16)$$

where $j_n = j_n(x=0)$ and $j_p = j_p(x=L)$ are the injection (or extraction) currents. Because the current at the boundaries is taken by either carrier, we must have

$$j = j_n = j_p \qquad (17)$$

In steady state (indicated by overbar), all the quantities are time independent (i.e., $\partial \bar{y}_k/\partial t = 0$) and we find that the occupation of the trap is given by

$$\bar{f} = \frac{\beta_n\bar{n} + \varepsilon_p}{\beta_n\bar{n} + \beta_p\bar{p} + \varepsilon_n + \varepsilon_p} \qquad (18)$$

In particular, at equilibrium:

$$f_0 = \frac{\beta_n n_0}{\beta_n n_0 + \varepsilon_n} = \frac{\varepsilon_p}{\beta_p p_0 + \varepsilon_p} \qquad (19)$$

Thus the current can be stated as

$$\bar{j} = qL(\bar{G} - \bar{U}_{SRH}) \qquad (20)$$

where

$$\bar{U}_{SRH} = N_t\beta_n\beta_p \frac{\bar{n}\bar{p} - n_i p_i}{\beta_n\bar{n} + \beta_p\bar{p} + \varepsilon_n + \varepsilon_p} \qquad (21)$$

is the standard SRH recombination rate.

By the structure of the solar cell device, the applied voltage or photovoltage is related to the above-defined voltages as

$$V_{app} = V_n - V_p \qquad (22)$$

The determination of the separate voltages as a function of the applied voltage, V_{app}, requires stating a relationship between the number of electrons and holes. In a homogeneous medium we have the condition of electroneutrality. Then, with a net background of doping of positive ionic charge N_{ion}^+ we obtain

$$n - p - N_{ion}^+ = 0 \qquad (23)$$

Equations 20−23 allow determining all steady state characteristics such as the current−voltage curve. In particular, eqs 22 and 23 allow one to express the densities of free electrons and holes (previously expressed according to eqs 7 and 8) as a function of the applied voltage V_{app} in the presence of a net density of positively charged dopant

$$n = \frac{1}{2}N_{ion}^+ \left\{ \left[1 + 4\left(\frac{n_i}{N_{ion}^+}\right)^2 e^{-qV_{app}/k_BT} \right]^{1/2} + 1 \right\} \qquad (24)$$

$$p = \frac{1}{2}N_{ion}^+ \left\{ \left[1 + 4\left(\frac{n_i}{N_{ion}^+}\right)^2 e^{-qV_{app}/k_BT} \right]^{1/2} - 1 \right\} \qquad (25)$$

Note that for an n-type semiconductor, the previous equations can be simplified at first order into

$$n \approx N_{ion}^+ \qquad (26)$$

$$p \approx \frac{n_i^2}{N_{ion}^+} e^{-qV_{app}/k_BT} \qquad (27)$$

These last equations are valid as long as $n(V_{app}) \gg p(V_{app})$.

In the calculation of the impedance, we use a small sinusoidal perturbation of voltage imposed over a steady state. The small signal is modulated with angular frequency ω so that we can use the substitution $\partial/\partial t \to i\omega$ to solve the equations in the Laplace domain. We can split all quantities as follows

$$y_k = \bar{y}_k + \hat{y}_k(t) \qquad (28)$$

$$j_k = \bar{j}_k + i_k(t) \qquad (29)$$

$$V_k = \bar{V}_k + v_k(t) \qquad (30)$$

The definition of the impedance is the ratio of modulated voltage to current, that is

$$Z = \frac{v_n - v_p}{i_{tot}} \qquad (31)$$

where $i_{tot} = i_n = i_p$. The equations for the modulated quantities are obtained by linear expansion of eqs 12, 15, and 16 with the following result

$$\frac{i_n}{qL} + [i\omega + \beta_n N_t(1 - \bar{f})]\hat{n} - (\beta_n \bar{n} + \varepsilon_n)N_t\hat{f} = 0 \qquad (32)$$

$$\frac{i_p}{qL} + [i\omega + \beta_p N_t \bar{f}]\hat{p} + (\beta_p \bar{p} + \varepsilon_p)N_t\hat{f} = 0 \qquad (33)$$

$$[i\omega + \beta_n \bar{n} + \varepsilon_n + \beta_p \bar{p} + \varepsilon_p]\hat{f} - \beta_n \hat{n}(1 - \bar{f}) + \beta_p \hat{p}\bar{f} = 0 \qquad (34)$$

We introduce the equilibrium chemical capacitances[13]

$$C_\mu^n = -qL\frac{\partial \bar{n}}{\partial \bar{V}_n} = \frac{q^2 L\bar{n}}{k_BT} \qquad (35)$$

$$C_\mu^p = qL\frac{\partial \bar{p}}{\partial \bar{V}_p} = \frac{q^2 L\bar{p}}{k_BT} \qquad (36)$$

$$C_\mu^t = -qL\frac{\partial \bar{f}}{\partial \bar{V}_t}N_t = \frac{q^2 L}{k_BT}\bar{f}(1 - \bar{f})N_t \qquad (37)$$

then we can write the following expressions for the modulated densities

$$\hat{n} = -\frac{C_\mu^n}{qL}v_n \qquad (38)$$

$$\hat{p} = \frac{C_\mu^p}{qL}v_p \qquad (39)$$

$$N_t\hat{f} = -\frac{C_\mu^t}{qL}v_t \qquad (40)$$

We define the following resistances[14−16]

$$R_{tn}^{-1} = C_\mu^n \beta_n N_t(1 - \bar{f}) = \frac{q^2 L}{kT}N_t\beta_n\bar{n}(1 - \bar{f}) \qquad (41)$$

$$R_{tp}^{-1} = C_\mu^p \beta_p N_t\bar{f} = \frac{q^2 L}{kT}N_t\beta_p\bar{p}\bar{f} \qquad (42)$$

$$R_{rec}^n{}^{-1} = R_{tn}^{-1} - C_\mu^t[\beta_n\bar{n} + \varepsilon_n] = \frac{q^2 L}{kT}(1 - \bar{f})\bar{U}_{SRH} \qquad (43)$$

$$R_{rec}^p{}^{-1} = R_{tp}^{-1} - C_\mu^t[\beta_p\bar{p} + \varepsilon_p] = \frac{q^2 L}{kT}\bar{f}\,\bar{U}_{SRH} \qquad (44)$$

It is also convenient to introduce admittances and conductances as follows

$$Y_\mu^k = i\omega C_\mu^k \qquad (45)$$

$$G_k = R_k^{-1} \qquad (46)$$

Then eqs 32−34 can be expressed in the form

$$i_n = Y_\mu^n v_n + G_{tn}(v_n - v_t) + G_{rec}^n v_t \qquad (47)$$

$$-i_p = Y_\mu^p v_p + G_{tp}(v_p - v_t) + G_{rec}^p v_t \qquad (48)$$

$$0 = G_{tn}(v_n - v_t) + G_{tp}(v_p - v_t) + (G_{rec}^n + G_{rec}^p - Y_\mu^t)v_t \qquad (49)$$

These three equations state the conservation of current and can be represented as an EC, shown in Figure 2.

This EC was derived by Shockley for the equilibrium situation and by Sah for the general case that we show here.[9,10] The left vertical branch is indicated as a current generator because the current depends on the voltage drop at the capacitor associated to the traps.

C

dx.doi.org/10.1021/jp411004e | J. Phys. Chem. C XXXX, XXX, XXX−XXX
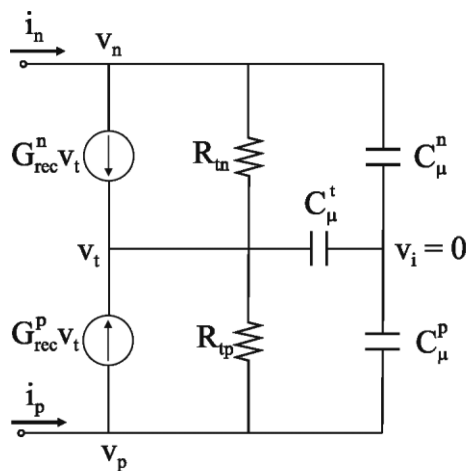
Figure 2. Equivalent circuit for the SRH recombination model. The electrical components of the EC are indicated along with the chemical potentials: v_n for electrons in the CB, v_p for holes in the VB, and v_t for traps. v_i is the intrinsic chemical potential.

Solving the linear system of eqs 47−49 we obtain the impedance as follows

$$Z = \frac{(Y_\mu^t + Y_\mu^n + Y_\mu^p)(G_{tp} + G_{tn}) - (G_{rec}^n + G_{rec}^p - Y_\mu^t)(Y_\mu^n + Y_\mu^p)}{\det}$$

(50)

where

$$\det = Y_\mu^n[G_{tp}(Y_\mu^p + Y_\mu^t - G_{rec}^n) - Y_\mu^p(G_{rec}^n + G_{rec}^p - Y_\mu^t)]$$
$$+ G_{tn}[G_{tp}(Y_\mu^t + Y_\mu^n + Y_\mu^p) + Y_\mu^p(Y_\mu^t + Y_\mu^n - G_{rec}^p)]$$

(51)

■ DISCUSSION

Before entering into the details of the practical application of the EC of Figure 2, it is useful to examine when it can be reduced to well-known reference cases.

The first case we discuss here is the impedance of the equilibrium steady state in which electrons and holes remain in dark equilibrium ($\bar{n} = n_0$, $\bar{p} = p_0$). This situation corresponds to the case depicted by Shockley.[9] The corresponding EC is given in Figure 3a. According to eqs 43 and 44, we have $G_{rec}^n = G_{rec}^p = 0$ and the current sources can be removed from the EC. Note that the conductance G_{tn} and G_{tp} can be simplified into

$$G_{tn} = \frac{q^2 L}{kT} N \vartheta_0 \, \varepsilon_n$$

(52)

$$G_{tp} = \frac{q^2 L}{kT} N \vartheta_0 \beta_p p_0$$

(53)

The total impedance is given by

(a)   (b)

(c)
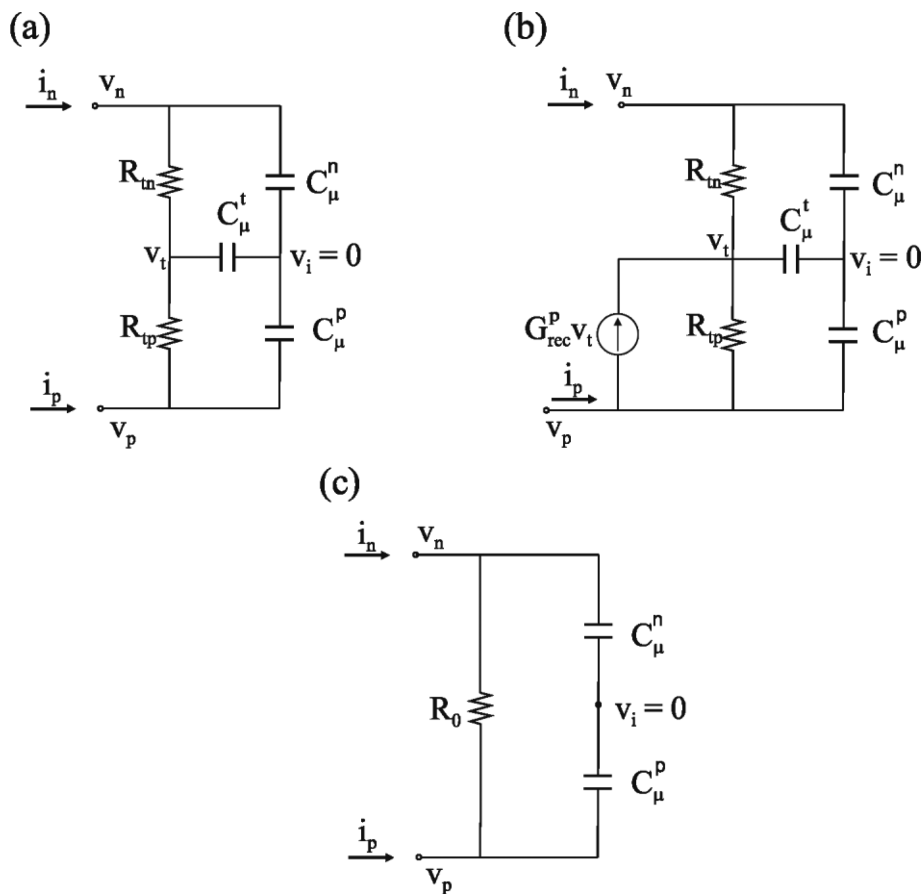
Figure 3. Reduction of the equivalent circuits of Figure 2 at equilibrium (a), for an n-type semiconductor (b) and in the absence of traps (c). In the latter case, a band-to-band recombination resistance R_0 has been introduced.

$$Z^a = \frac{(Y_\mu^t + Y_\mu^n + Y_\mu^p)(G_{tp} + G_{tn}) + Y_\mu^t(Y_\mu^n + Y_\mu^p)}{Y_\mu^n[Y_\mu^p Y_\mu^t + G_{tp}(Y_\mu^p + Y_\mu^t)] + G_{tn}[G_{tp}Y_\mu^p + (Y_\mu^p + G_{tp})(Y_\mu^t + Y_\mu^n)]}$$

(54)

The second case that we shall discuss is the presence of a majority carrier. Let us take the example of an n-type semiconductor.

$$Z^b = \frac{(Y_\mu^t + Y_\mu^n + Y_\mu^p)(G_{tp} + G_{tn}) - (G_{rec}^p - Y_\mu^t)(Y_\mu^n + Y_\mu^p)}{Y_\mu^n[G_{tp}(Y_\mu^p + Y_\mu^t) + Y_\mu^p(Y_\mu^t - G_{rec}^p)] + G_{tn}[G_{tp}(Y_\mu^t + Y_\mu^n + Y_\mu^p) + Y_\mu^p(Y_\mu^t + Y_\mu^n - G_{rec}^p)]}$$

(55)

This scenario is depicted by the EC of Figure 3b in which the current source associated to electrons in the conduction band has been removed. The upper part of the circuit associated to majority carrier corresponds to the equilibrium situation depicted by Shockley. Therefore majority carriers behave as if they were at equilibrium. Obviously this statement is true only if the applied voltage is such that the electron concentration remains much higher than the holes concentration.

The last case that we examine hereafter is the absence of traps ($N_t = 0$). In this configuration, all the conductances are zero and only remains the capacitances of electrons (C_μ^n) and holes (C_μ^p). Since there is no trap assisted recombination, band to band recombination occurs, as discussed by Garcia-Belmonte et al.[11] It is consequently necessary to introduce other conductances associated to band to band electrons and holes recombination as follows

$$G_{rec}^n = -qL\frac{\partial U_{np}}{\partial V_n}$$

(56)

$$G_{rec}^p = qL\frac{\partial U_{np}}{\partial V_p}$$

(57)

In eqs 56 and 57, U_{np} corresponds to the rate of band to band electron hole recombination. The corresponding EC is given in Figure 3c and the associated impedance can be written as follows

$$Z^c = \frac{Y_\mu^n + Y_\mu^p}{Y_\mu^p Y_\mu^n + Y_\mu^p G_{rec}^n + Y_\mu^n G_{rec}^p} = \frac{1}{R_0^{-1} + i\omega C_\mu^{eff}}$$

(58)

where

$$R_0 = \frac{C_\mu^n + C_\mu^p}{C_\mu^p G_{rec}^n + C_\mu^n G_{rec}^p}$$

(59)

$$C_\mu^{eff} = \frac{C_\mu^p C_\mu^n}{C_\mu^n + C_\mu^p}$$

(60)

We shall now examine in further details the practical use of the general equivalent circuit of Figure 2. Two issues of particular interests will be addressed in the following. The first one is related to the required conditions for the observation of two semicircles impedance spectra. It should be pointed out that in the vast majority of cases of IS measurements of solar cells only one recombination semicircle is observed. In fact, one single example where both carriers show a distinct spectral footprint has been reported to the best of our knowledge.[17] The second issue involves the necessity to take into account the current source of the EC of Figure 2 or whether it can be omitted to simplify the treatment of experimental data.

In this situation, the electron concentration in the CB does not vary with the applied voltage and $\bar{n} \approx N_{ion}^+$, as indicated by eq 26. A recombination center situated below the equilibrium Fermi level remains occupied by electrons ($f \approx 1$). In this case $G_{rec}^n \approx 0$ and the total impedance becomes

We first examine when two semicircles can be observed. To do so we shall distinguish between two extreme cases: small and large trap capacitance. Indeed, the trap capacitor actuates as an interrupter: when the trap capacitance is small, it behaves as an infinite resistance (open circuit) while if it is large, the trap capacitance behaves as a wire (short circuit). Note that the trap chemical capacitance reaches its maximum in the intrinsic regime, that is, when the population of electrons and holes are equal, and saturates at this value, contrary to the case of a unipolar semiconductor where the trap capacitance displays a
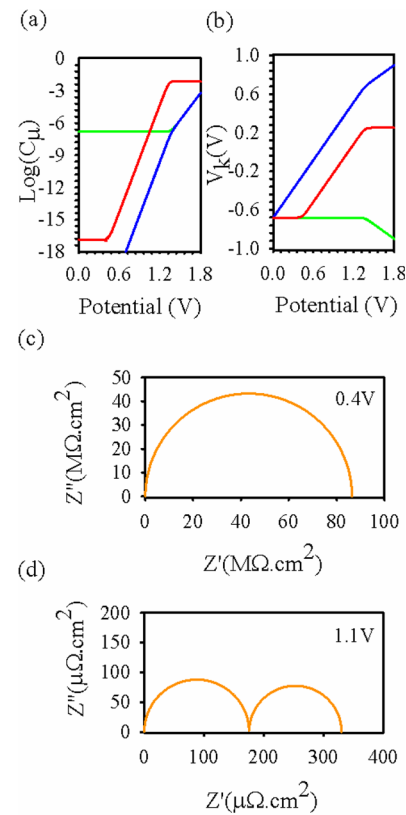
Figure 4. (a) Evolution with voltage of the chemical capacitances associated to the tree storage modes of an n-type semiconductor: conduction band (C_μ^n) (green plain line), valence band (C_μ^p) (blue plain line), and traps (C_μ^t) (red plain line). (b) Evolution of the corresponding electrochemical potentials: V_n (green plain line), V_p (blue plain line), and V_t (red plain line). (c) Impedance spectra obtained at 0.4 V, that is, when $C_\mu^p \ll C_\mu^n$. In this condition, the EC of Figure 5a can be applied to account for the semicircle observed in this impedance spectrum. (d) Impedance spectra obtained at 1.1 V, that is, when $C_\mu^t \gg C_\mu^n, C_\mu^p$. Under this condition, the EC of Figure 5b can be applied. Parameters of the simulation: $N_t = N_v = N_c = 10^{20}$ cm^{-3}, $\beta_n = \beta_p = 10^5$ cm^{-3} s^{-1}, $E_t = -0.25$ eV, $E_v = -1$ eV, $E_c = 1$ eV and $N_{ion} = 10^{15}$ cm^{-3}.

peak (see Figure 4a). Also note that the chemical capacitances follow the evolution of the corresponding electrochemical potentials, as depicted by Figure 4b. At low voltages, traps are filled by electrons and the chemical potential of traps follows the one of electrons. Because we simulated the case of an n-type semiconductor, the electrochemical potential of electrons is constant within a given range of voltage (for V_{app} < 1.4 V here). Therefore when voltage is increased, the chemical potential of holes first increases with voltage. When the latter chemical potential is sufficiently high to fill traps with a substantial quantity of holes, the chemical potential of traps starts increasing along with the holes chemical potential (at around V_{app} = 0.5 V). Once voltage is sufficiently high (V_{app} > 1.4 V), both the chemical potential of electrons and holes vary at the same rate (intrinsic regime) and the system becomes ambipolar. In this case, traps are equally filled by electrons and holes and the traps electrochemical potential does not vary with voltage.

In the case of a small trap capacitance, the EC of Figure 2 can be reduced to the one of Figure 5a and the valence and
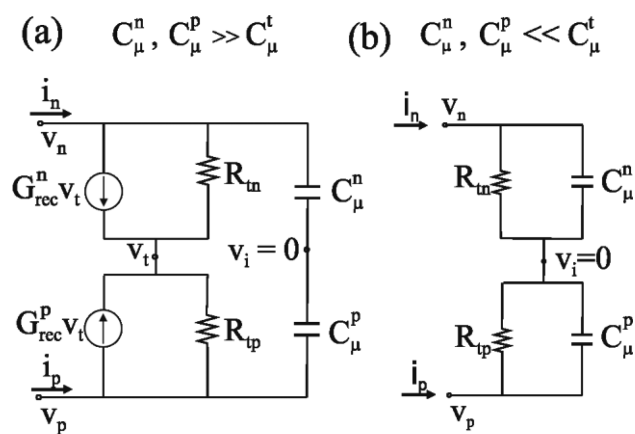
Figure 5. Reduction of the EC of Figure 2 when the trap capacitance is much smaller (a) or larger (b) than that of the conduction and valence bands. In the case of a small trap capacitance, one single semicircle can be observed in the IS spectra while for a large trap capacitance, the current sources are short-circuited and two semicircles may be observed, as detailed in the text.

conduction band capacitances are in series. In this configuration, the IS spectra will be featured by one single semicircle, as indicated by the example of Figure 4c. In the case of a large trap capacitance, the equivalent circuit can be reduced to the one of Figure 5b, which generates two semicircles associated to the capacitances of electrons and holes as depicted by the example of Figure 4d. Both semicircles will be distinguishable if the trapping times associated to electrons and holes are different enough and the trapping resistances similar. It is worth remarking that for an intrinsic semiconductor trapping lifetimes only depend on the position of the traps in the band gap and are usually very similar. As a result, both semicircles will never be neatly distinguishable for an intrinsic semiconductor, unlike for an extrinsic semiconductor where the chemical capacitances of the majority and minority carriers differ by several orders of magnitude.

For the sake of the practical analysis of the IS spectra, we shall now discuss the second point, that is whether the current sources can be removed from the EC of Figure 2. As mentioned above, when the trap capacitance is higher than the one of the

valence and conduction bands, the current sources are short circuited. The role of the current sources should therefore be discussed when the trap chemical capacitance is inferior to those of free electrons and holes.

In Figure 6, we give two examples of impedance spectra corresponding to an intrinsic semiconductor (Figure 6a) and to
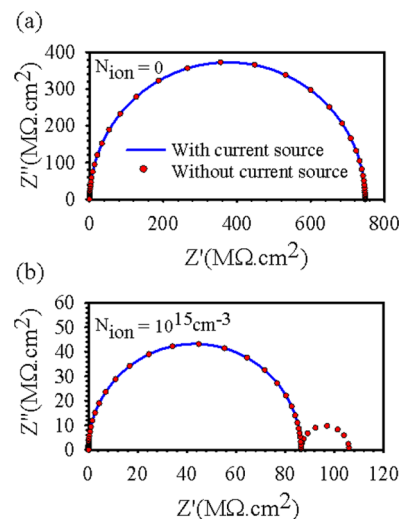
Figure 6. IS spectra simulated at applied voltage V_{app} = 0.4 V with the impedance given by eqs 50 and 51 (blue plain line) and by taking off the terms corresponding to the current sources (i.e., G_{rec}^n and G_{rec}^p) (red dots) in the case of an intrinsic semiconductor (a) and an n-type semiconductor (b). For the simulation of the intrinsic case (a), we used $N_t = 10^7 \text{cm}^{-3}$ and $\beta_n = \beta_p = 1 \text{ cm}^{-3} \text{ s}^{-1}$ in order to impose $C_\mu^t \ll C_\mu^n, C_\mu^p$. The rest of the parameters are the same as the one of Figure 4.

an n-type semiconductor (Figure 6b). From these plots, it is clear that for an intrinsic semiconductor the current sources can be removed, in contrast to the case of an extrinsic semiconductor. Indeed, in the case of an intrinsic semiconductor the total resistance (i.e., $Z(\omega = 0)$) is independent of the conductances associated to the current sources (G_{rec}^n and G_{rec}^p) and our simulations show that at higher frequencies, the error committed by omitting the current sources remains negligible. For the case of an extrinsic semiconductor, the current sources appear to be of prime interest. Omitting them is equivalent to short circuit them and consequently impose that the trap capacitance is much larger than the free carrier chemical capacitances for any applied voltage, leading to the presence of two possible semicircles in the IS spectra, as shown in Figure 6b (red dots).

■ CONCLUSION

We have calculated the complex impedance for an ambipolar solar cell subject to trap-mediated recombination. We have recovered the EC already obtained by Shockley in the case of the perturbation of an equilibrium steady state and by Sah for a steady state off equilibrium. After reducing the latter circuit to some well-known cases (presence of a majority carrier, equilibrium steady state and absence of traps), we have shown that it is possible to obtain two semicircles if the trap capacitance is larger than the one of the conduction and valence bands. Extrinsic semiconductors have been shown to display neater semicircles than intrinsic semiconductors due to the large difference between the chemical capacitances of the minority and majority carriers. The role of the current sources

in the general EC has been examined. It has been inferred from our study that for an intrinsic semiconductor, the current sources can be removed from the EC, though not for extrinsic semiconductors.

■ AUTHOR INFORMATION

Corresponding Author

*E-mail: bisquert@uji.es.

Notes

The authors declare no competing financial interest.

■ ACKNOWLEDGMENTS

■ REFERENCES

(1) Bisquert, J.; Cahen, D.; Rühle, S.; Hodes, G.; Zaban, A. Physical Chemical Principles of Photovoltaic Conversion with Nanoparticulate, Mesoporous Dye-Sensitized Solar Cells. *J. Phys. Chem. B* **2004**, *108*, 8106−8118.

(2) van Roosbroeck, W. The Transport of Added Current Carriers in a Homogeneous Semiconductor. *Phys. Rev.* **1953**, *91*, 282−289.

(3) Tang, J.; Wang, X.; Brzozowski, L.; Barkhouse, D. A. R.; Debnath, R.; Levina, L.; Sargent, E. H. Schottky Quantum Dot Solar Cells Stable in Air Under Solar Illumination. *Adv. Mater.* **2011**, *22*, 1398−1402.

(4) Kim, H.-S.; Lee, C.-R.; Im, J.-H.; Lee, K.-B.; Moehl, T.; Marchioro, A.; Moon, S.-J.; Humphry-Baker, R.; Yum, J.-H.; Moser, J. E.; Grätzel, M.; Park, N.-G. Lead Iodide Perovskite Sensitized All-Solid-State Submicron Thin Film Mesoscopic Solar Cell with Efficiency Exceeding 9%. *Sci. Rep.* **2012**, *2*, 591.

(5) Lee, M. M.; Teuscher, J.; Miyasaka, T.; Murakami, T. N.; Snaith, H. J. Efficient Hybrid Solar Cells Based on Meso-Superstructured Organometal Halide Perovskites. *Science* **2012**, *338*, 643−647.

(6) Fabregat-Santiago, F.; Garcia-Belmonte, G.; Mora-Seró, I.; Bisquert, J. Characterization of Nanostructured Hybrid and Organic Solar Cells by Impedance Spectroscopy. *Phys. Chem. Chem. Phys.* **2011**, *13*, 9083−9118.

(7) Bisquert, J. Theory of the Impedance of Electron Diffusion and Recombination in a Thin Layer. *J. Phys. Chem. B* **2002**, *106*, 325−333.

(8) Bisquert, J.; Mora-Sero, I.; Fabregat-Santiago, F. Diffusion-Recombination Impedance Model for Solar Cells with Disorder and Nonlinear Recombination. *ChemElectroChem* **2013**, DOI: 10.1002/celc.201300091.

(9) Shockley, W. Electrons, Holes, and Traps. *Proc. IRE* **1958**, *46*, 973−990.

(10) Sah, C.-T. The Equivalent Circuit Model in Solid State Electronics–Part I: The Single Energy Level Defect Centers. *Proc. IEEE* **1967**, *55*, 654−671.

(11) Garcia-Belmonte, G.; Boix, P. P.; Bisquert, J.; Sessolo, M.; Bolink, H. J. Simultaneous Determination of Carrier Lifetime and Electron Density-of-States in P3HT:PCBM Organic Solar Cells Under Illumination by Impedance Spectroscopy. *Sol. Energy Mater. Sol. Cells* **2010**, *94*, 366−375.

(12) Shockley, W.; Read, W. T. Statistics of the Recombinations of Holes and Electrons. *Phys. Rev.* **1952**, *87*, 835−842.

(13) Bisquert, J. Chemical Capacitance of Nanostructured Semiconductors: Its Origin and Significance for Heterogeneous Solar Cells. *Phys. Chem. Chem. Phys.* **2003**, *5*, 5360−5364.

(14) Bisquert, J. Beyond the Quasi-Static Approximation: Impedance and Capacitance of an Exponential Distribution of Traps. *Phys. Rev. B* **2008**, *77*, 235203.

(15) Bisquert, J. Theory of the Impedance of Charge Transfer via Surface States in Dye-Sensitized Solar Cells. *J. Electroanal. Chem.* **2010**, *646*, 43−51.

(16) Bertoluzzi, L.; Bisquert, J. Equivalent Circuit of Electrons and Holes in Thin Semiconductor Films for Photoelectrochemical Water Splitting Applications. *J. Phys. Chem. Lett.* **2012**, *3*, 2517−2522.

(17) Mora-Seró, I.; Luo, Y.; Garcia-Belmonte, G.; Bisquert, J.; Muñoz, D.; Voz, C.; Puigdollers, J.; Alcubilla, R. Recombination Rates in Heterojunction Silicon Solar Cells Analyzed By Impedance Spectroscopy at Forward Bias and Under Illumination. *Sol. Energy Mater. Sol. Cells* **2008**, *92*, 505−509.